ISSN: 2277-9655
Impact Factor: 4.116
CODEN: IJESS7

IJESRT

INTERNATIONAL JOURNAL OF ENGINEERING SCIENCES & RESEARCH TECHNOLOGY

TO STUDY AND ANALYSIS OF A MICRO MECHANICAL MODEL OF TWO DIFFERENT HARD STEEL OF DIFFERENT COMPOSITION BY VOLUME ELEMENT METHOD

Harshita Gupta*, Anshuka Srivastava, Prabhat Kumar Sinha
* M.Tech. Scholar, Dept. of Mechanical Engineering, SHIATS, Allahabad, U.P., India
Professor, Dept. of Mechanical Engineering, SHIATS Allahabad, U.P., India
Assistant Professor, Dept. of Mechanical Engineering, SHIATS Allahabad, U.P., India

DOI: 10.5281/zenodo.154561

ABSTRACT

This work presented the Micromechanical modeling of flow curve of DP800 steel in uniaxial tension was studied using the representative volume element (RVE) method. Digimat and ABAQUS software were coupled and used to provide the required RVE model parameters and to perform simulations. Modeling results were validated using the experimental flow curves of the steels. It was found that the flow curve of DP800 steel was accurately predicted from the onset of plastic deformation up to the onset of necking. The RVE size of 12.7x12.7x12.7 μm and 7.9x7.9x7.9 μm containing 26 martensite islands were found as the optimum RVE sizes for DP800 steel. A mesh of C3D4 elements having a size of 0.050 μm was found to be the optimum element type and mesh.

KEYWORDS: DP800 steel, representative volume element (RVE) method, ABAQUS software, flow curves of the steels, onset of necking, optimum element type and mesh.

INTRODUCTION

Dual phase steels introduced in the 1960s and started to be used in the manufacturing industry in the 1970s. Their greater combination of strength and ductility compared to conventional steels encouraged the industries to support research on processing and microstructure-properties relationship of dual phase steels. The microstructure of dual phase steels consists of ferrite as the soft matrix and martensite as the hard phase, and small amounts of bainite may also be present. Ferrite and martensite are responsible for plastic deformation and strengthening of dual phase steels, respectively.

Commercial dual phase steels are produced by an intercritical annealing heat treatment in the ($\alpha + \Upsilon$) region of the iron-cementite phase diagram followed by rapid quenching to room temperature. Quenching must be sufficiently fast to avoid the diffusion and formation of other structures such as pearlite and bainite. However, in bainite-assisted dual phase steel, the steel is quenched to a certain temperature, an isothermal heat treatment is carried out to form bainite and a second rapid quench cools the steel to room temperature. The martensite volume fraction varies in different grades of dual phase steel.The martensite fraction in a typical DP800 and DP780 steel is approximately 10 vol% and 20 vol%, respectively; however, in a DP980 steel, the volume fraction of martensite is more than 30 vol% in order to provide sufficient strength to the steel. The martensite content in dual phase steels determines the intercritical annealing temperature. According to the lever rule, greater amounts of austenite are formed at higher intercritical annealing temperatures which transforms to martensite by rapid quenching.

During processing of dual phase steels, different alloying elements are used in solid solution to increase the strength and hardness of the steel. Silicon, manganese, chromium, and molybdenum are the typical alloying elements in dual phase steels. Silicon affects the chemical composition of austenite by accelerating the migration of carbon atoms from the ferrite to the austenite during intercritical annealing. Manganese is used to enhance hardenability of dual phase steels. Chromium and molybdenum reduce the critical cooling rate of austenite for martensitic transformation. Other elements such as vanadium and titanium may be added to form carbide and nitride precipitates that can increase the strength of the steel by precipitation hardening. These precipitates limit the movement of the ferrite-austenite interface during quenching and enhance the martensite formation.

ISSN: 2277-9655
Impact Factor: 4.116
CODEN: IJESS7

Motivations for Dual Phase Steels

Most of the current passenger vehicles operate on fossil fuels which tend to create economic and ecological challenges. One way to decrease fuel consumption is to reduce vehicle weight and this can be done by using stronger and thinner sheets in the vehicle body so as not to compromise passenger safety. Reducing the thickness of body parts and simultaneously preserving occupant safety requires a grade of sheet metal with an excellent combination of strength and formability such as dual phase steels.

Strengthening Mechanisms in Dual Phase Steels

The microstructure of commercial dual phase steels includes ferrite and martensite. Depending on the heat treatment cycle, it may also include same bainite. The influence of strengthening mechanisms in ferrite, martensite and bainite on the flow stress of dual phase steels is discussed in the following.

Ferrite

Ferrite is the interstitial solid solution of carbon in body centered cubic (BCC) iron. It is the predominant phase in most low carbon steels including high strength low alloy steels (HSLA) and dual phase steels (DP). The ferrite grain size has a significant influence on the yield strength of dual phase steels. The influence of grain size on yield strength is described by the Hall-Petch relationship which was successively developed by Hall and then Petch:

$$\sigma_y = \sigma_o \, ky \, d^{1/2}$$

where d is the grain diameter, σ_y is the yield stress, σ_0 is the friction stress opposing the movement of dislocations in the grains and k_y is a constant. The mean ferrite grain size in advanced dual phase steels is reduced to less than 10 µm which remarkably enhances the flow stress. Solid solution hardening is another strengthening mechanism that enhances the flow stress of ferrite. In dual phase steels, manganese is the dominant alloying element which has a notable influence on strengthening of the steel. Solid solution strengthening depends on the solute concentration as follows: $\sigma_{SSS} = kc^n$
where c is the solute concentration, k is a constant, and $0.5<n<0.67$.

Martensite

During processing of dual phase steels, the steel is quenched from the intercritical annealing temperature to room temperature. During this heat treatment, the intercritical austenite transforms to martensite by a diffusionless phase transformation. The mechanical strength of martensite primarily depends on its carbon content. The dependence of martensite hardness on the carbon content of the steel is shown in Figure 1-1. Also, Figure 1-2 presents the yield strength of martensite as a function of martensite carbon content. Similar to ferrite, solid solution hardening is a strengthening mechanism in martensite.

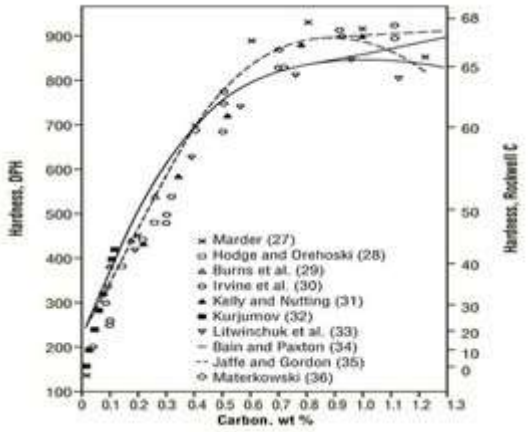

Figure 1 -1 Hardness of martensitic steel as a function of carbon content

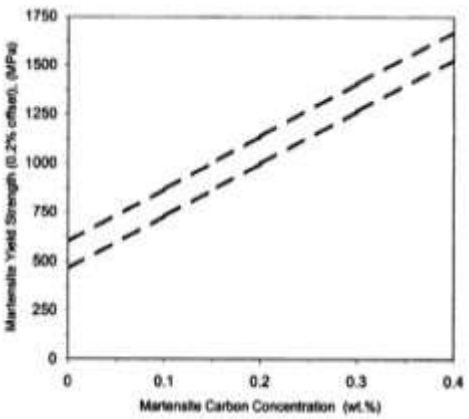

Figure 1 -2 Dependence of martensite yield strength on martensite carbon content

DP800 Dual Phase Steel

According to the quantitative metallography results, the martensite volume fraction in DP800 steel was 0.090. Based on the martensite content, the aspect ratio of martensite islands and the martensite size distribution in DP800 steel, 6 RVEs with different sizes were generated. Since both the morphology and the volume fraction of

ISSN: 2277-9655
Impact Factor: 4.116
CODEN: IJESS7

martensite were considered in RVE generation, all of the 6 RVEs properly presented the overall microstructural characteristics of the steel. Hence, as can be seen in Figure 1-3 to Figure 1-4, the predicted flow curves are generally very close to the experimental flow curve.

Table 3-1 Specifications of the RVEs generated for micromechanical modeling of DP800 steel

RVE Size Cube Side (µm)	Number of Martensite islands inside the RVE	Effective volume Fraction of Martensite inside the RVE	Modeling Results
9.5	11	0.090	Figure 1-3
10.3	14	0.089	Figure 1-4
11.6	20	0.091	Figure 1-5
12.7	26	0.090	Figure 1-6
13.2	29	0.090	Figure 1-7
14.2	36	0.096	Figure 1-8

As it can be seen in Figure 1-6(f), Figure 1-7(f) and Figure 1-8(f), when the number of martensite islands inside an RVE is more than 25, the numerical flow curve practically lies on the experimental flow curve. While the ultimate tensile strength (UTS) in the experimental flow curve is 648.7 MPa, the RVEs with 26, 29 and 36 martensite islands predict an ultimate tensile strength of 649.0, 649.6 and 646.8 MPa, respectively. Hence, the error is less than 0.3%. When the number of martensite islands in the RVEs was 11, 14 and 20, the numerical flow curve underestimated the flow stress of DP800 steel. The predicted ultimate tensile strengths by the RVEs including 11, 14 and 20 martensite islands were 637.4, 647.6 and 632.1 MPa, respectively. Compared to the RVEs with more than 25 martensite islands, since the number of martensite islands inside of RVEs with 11, 14 and 20 martensite islands was not sufficient, the size distribution of martensite in the RVE was not sufficiently similar to the size distribution of martensite in the real microstructure. Hence, these smaller RVEs could not properly represent the characteristics of the microstructure.

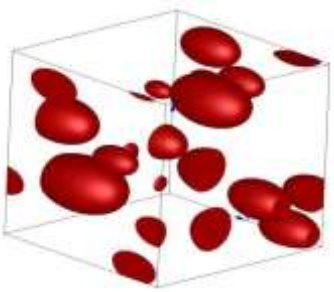

(a)

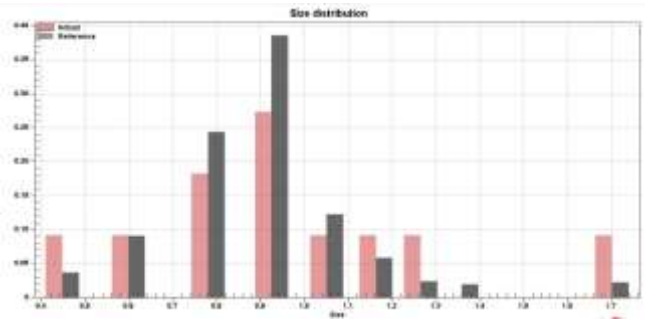

(b)

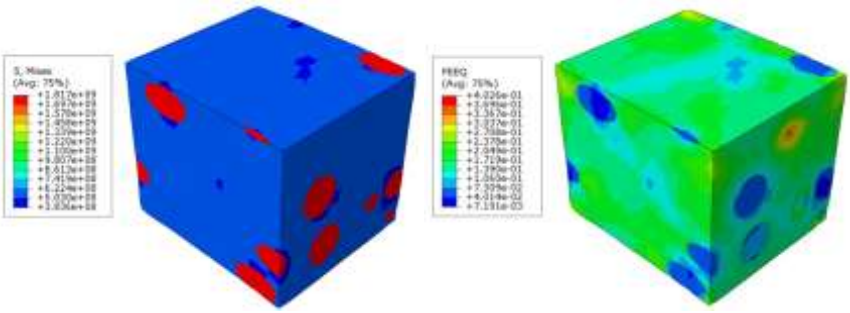

(c) ***(d)***

ISSN: 2277-9655
Impact Factor: 4.116
CODEN: IJESS7

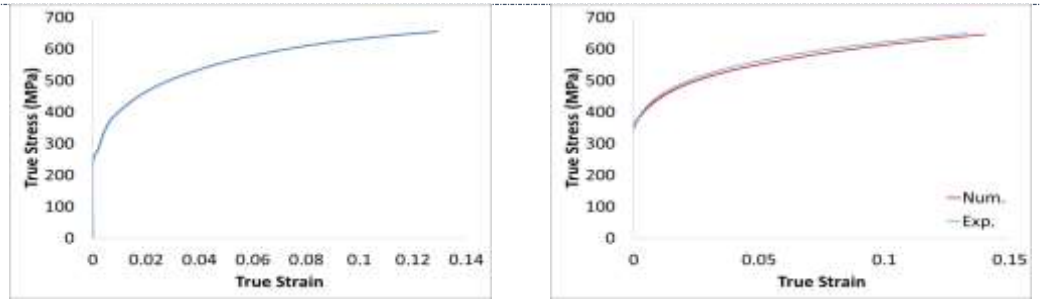

(e) *(f)*

Figure 1-3 Micromechanical modeling results for DP800 steel with 11 martensite islands inside the RVE: (a) RVE, (b) distribution of martensite in the RVE, (c) distribution of von Mises stress in the RVE at ε≈0.12, (d) distribution of equivalent strain in the RVE at ε≈0.14, (e) flow curve of RVE and (f) numerical and experimental flow curves of DP800 steel.

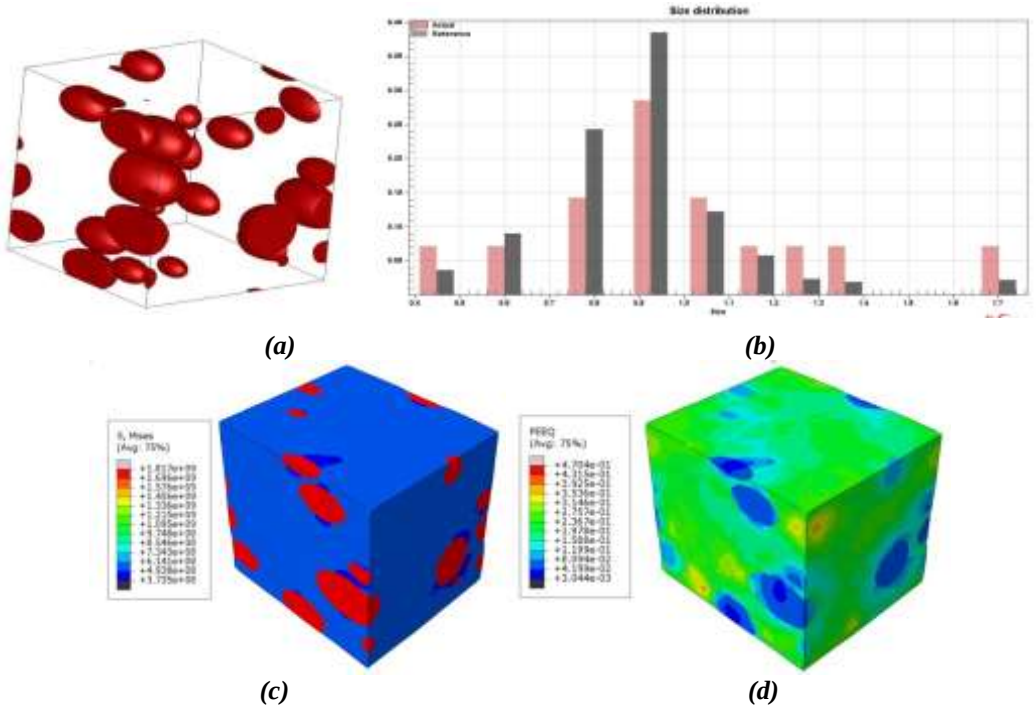

(a) *(b)*

(c) *(d)*

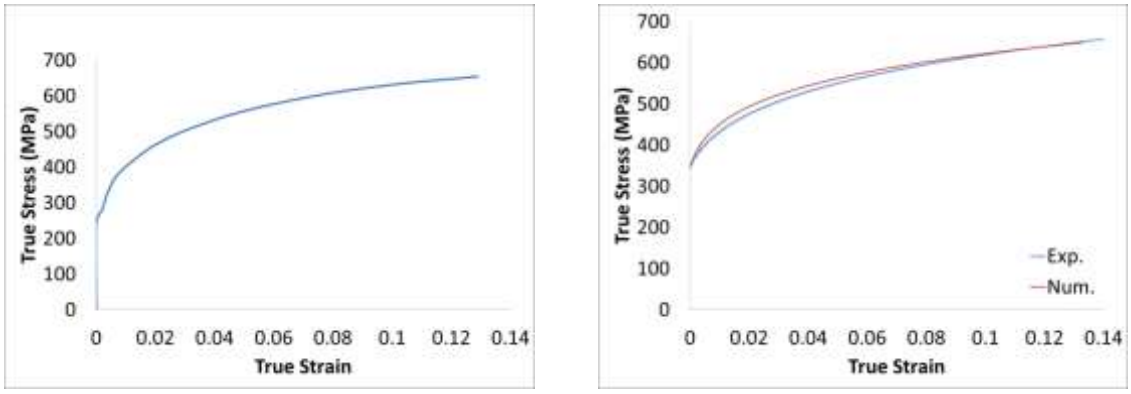

(e) *(f)*

Figure 1-4 Micromechanical modeling results for DP800 steel with 14 martensite islands inside the RVE: (a) RVE, (b) distribution of martensite in the RVE, (c) distribution of von Mises stress in the RVE at ε≈0.12,

ISSN: 2277-9655
Impact Factor: 4.116
CODEN: IJESS7

(d) distribution of equivalent strain in the RVE at ε≈0.14, (e) flow curve of RVE and (f) numerical and experimental flow curves of DP800 steel.

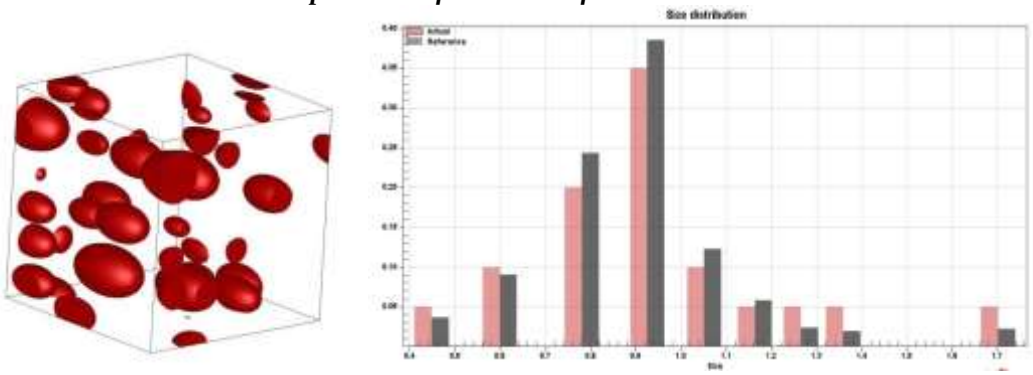

(a) *(b)*

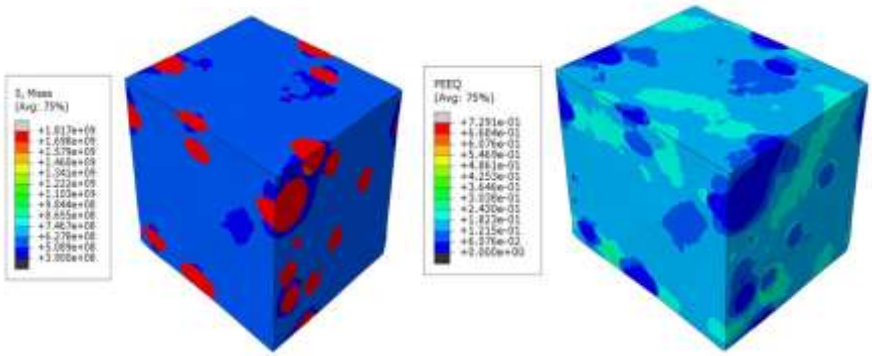

(c) *(d)*

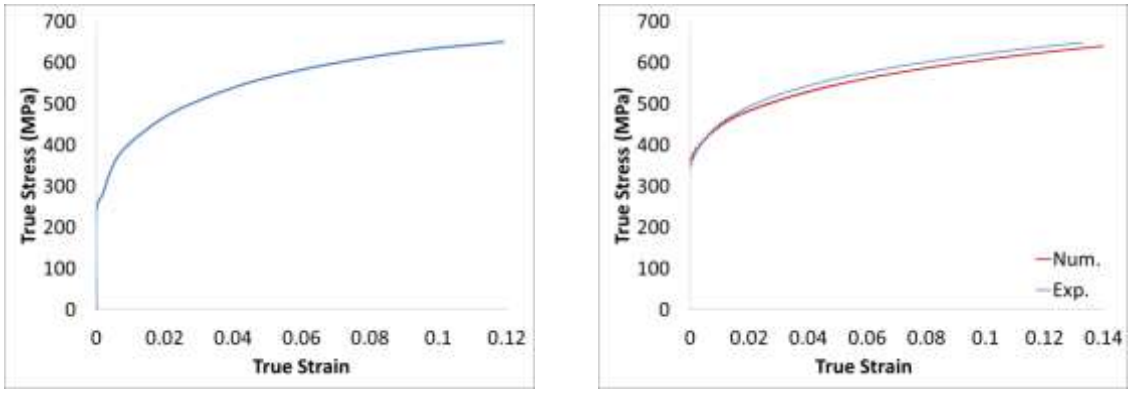

(e) *(f)*

Figure 1-5 Micromechanical modeling results for DP800 steel with 20 martensite islands inside the RVE: (a) RVE, (b) distribution of martensite in the RVE, (c) distribution of von Mises stress in the RVE at ε≈0.12, (d) distribution of equivalent strain in the RVE at ε≈0.14, (e) flow curve of RVE and (f) numerical and experimental flow curves of DP800 steel.

ISSN: 2277-9655
Impact Factor: 4.116
CODEN: IJESS7

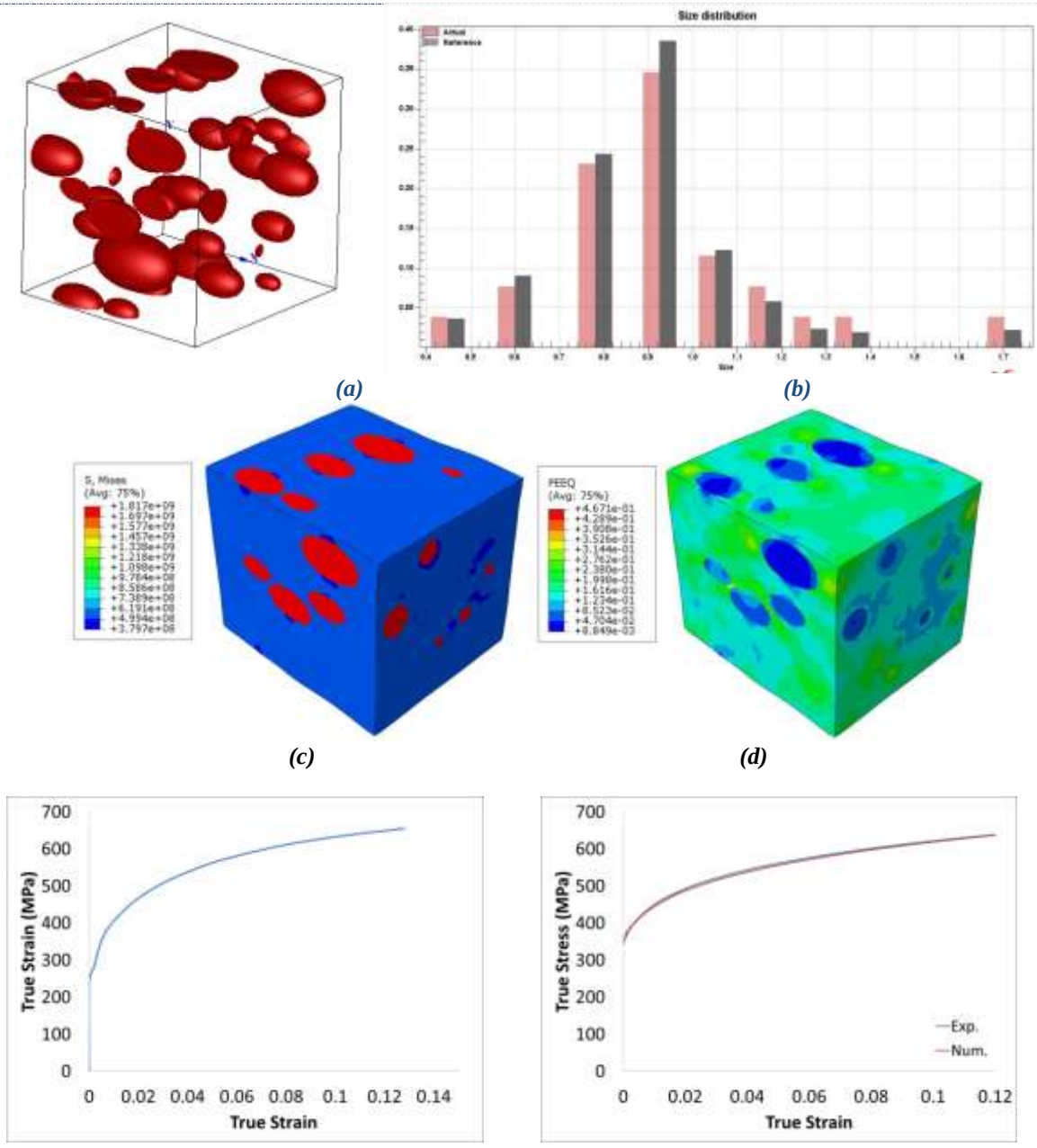

Figure 1-6 Micromechanical modeling results for DP800 steel with 26 martensite islands inside the RVE: (a) RVE, (b) distribution of martensite in the RVE, (c) distribution of von Mises stress in the RVE at ε≈0.12, (d) distribution of equivalent strain in the RVE at ε≈0.14, (e) flow curve of RVE and (f) numerical and experimental flow curves of DP800 steel.

ISSN: 2277-9655
Impact Factor: 4.116
CODEN: IJESS7

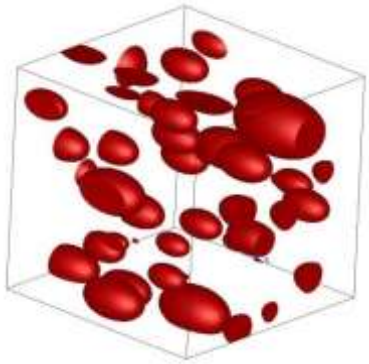

(a)

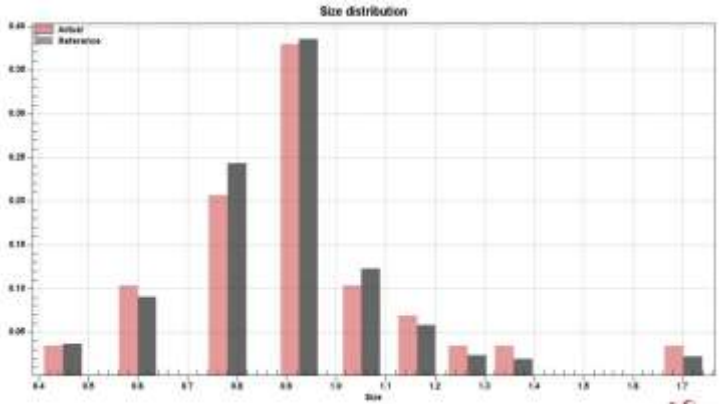

(b)

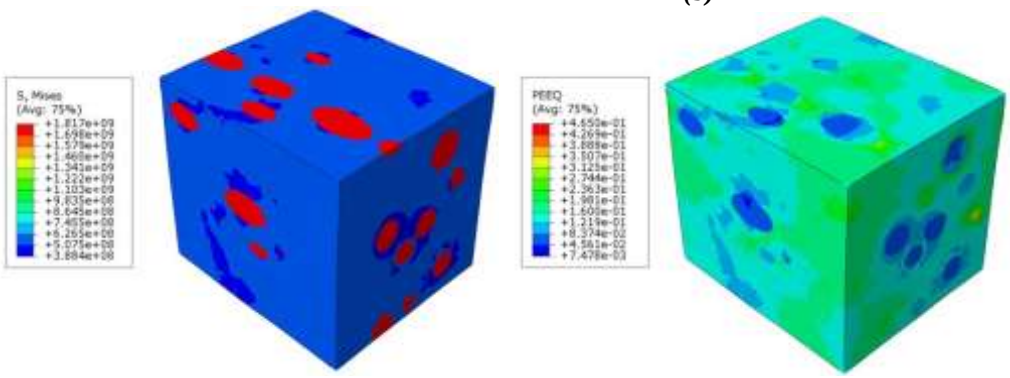

(c) (d)

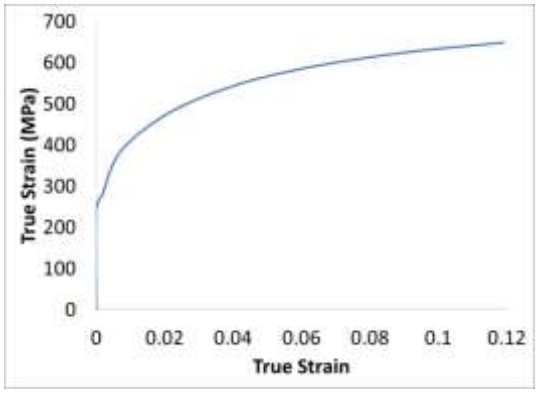

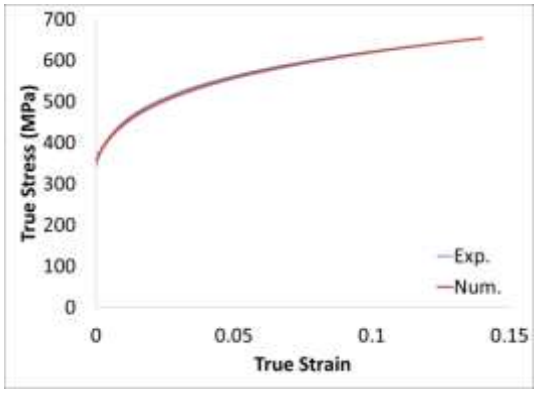

(e) (f)

Figure 1-7 Micromechanical modeling results for DP800 steel with 29 martensite islands inside the RVE: (a) RVE, (b) distribution of martensite in the RVE, (c) distribution of von Mises stress in the RVE at ε≈0.12, (d) distribution of equivalent strain in the RVE at ε≈0.14, (e) flow curve of RVE and (f) numerical and experimental flow curves of DP800 steel.

ISSN: 2277-9655
Impact Factor: 4.116
CODEN: IJESS7

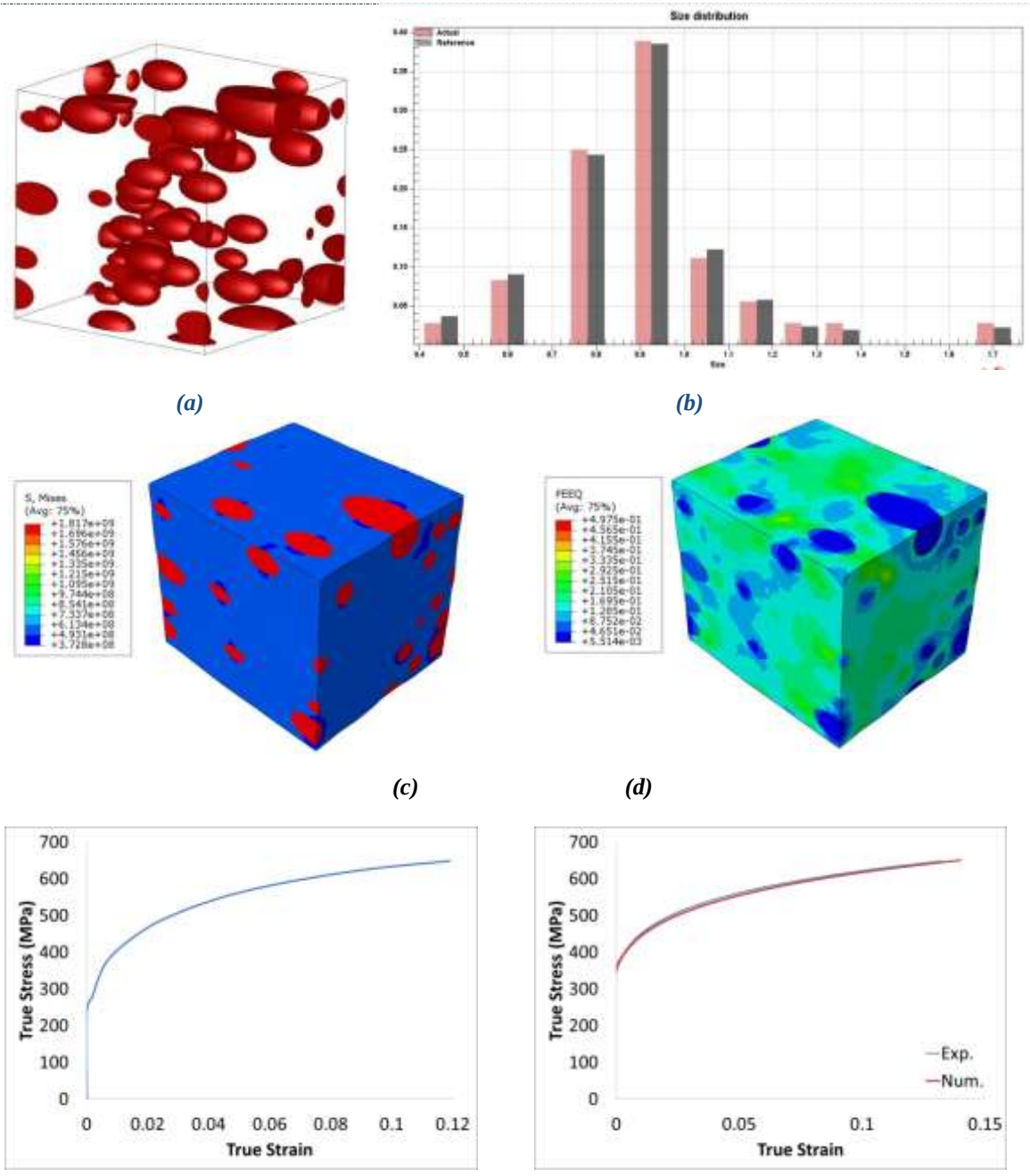

Figure 1-8 Micromechanical modeling results for DP800 steel with 36 martensite islands inside the RVE: (a) RVE, (b) distribution of martensite in the RVE, (c) distribution of von Mises stress in the RVE at ε≈0.12, (d) distribution of equivalent strain in the RVE at ε≈0.14, (e) flow curve of RVE and (f) numerical and experimental flow curves of DP800 steel.

The accuracy of the predicted flow curves, the experimental and predicted tensile toughness of the DP800 steel, i.e. the area below the flow curves, were compared. The predicted toughness of the steel was numerically calculated using more than 2000 data points. As it is shown in Figure 1-9(a), all the RVEs predicted the toughness of the steel quite accurately. For a more precise comparison, the results of Figure 1-9(a) are shown in Figure 1-9(b) with a magnified scale. As it can be seen, the RVEs with a size of 9.5, 10.3 and 11.6 μm^3, underestimated the toughness of the steel more than the RVEs with a size of equal to or greater than 12.7 μm. Comparing the modeling results for the DP800 flow curve, the accuracy of modeling results using RVEs with a size of 12.7, 13.2 and 14.2 μm^3 and with 26, 29 and 36 martensite islands, respectively, was almost similar; however,

ISSN: 2277-9655
Impact Factor: 4.116
CODEN: IJESS7

modeling time for the RVEs with 29 and 36 martensite islands is notably longer than the required modeling time for the RVE with 26 martensite islands. Therefore, an RVE size of 12.7x12.7x12.7 μm^3 containing 26 martensite islands is suggested as the optimum RVE size since it accurately predicted the flow curve of this DP800 steel. As can be seen in Figure 1-6(b), when the number of martensite islands was 26, it was feasible for the Digimat software to generate an RVE with a martensite size distribution similar to the martensite size distribution in the real microstructure.

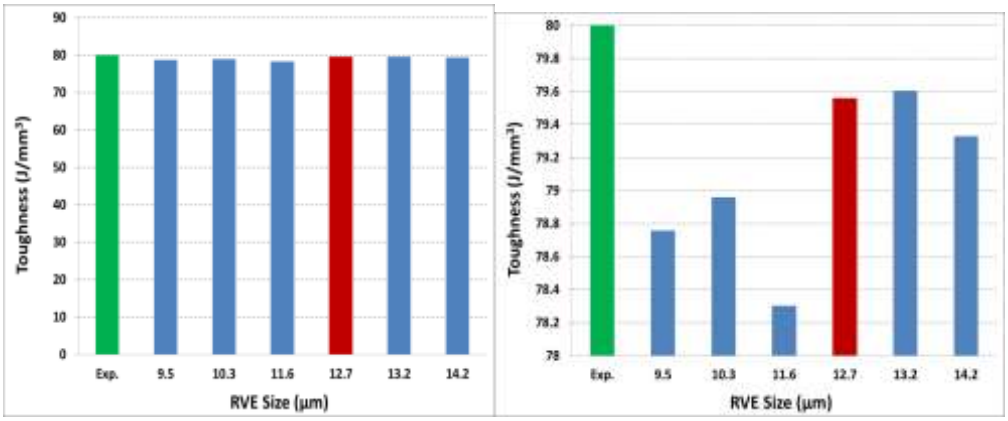

Figure 1-9 (a) Tensile toughness of the DP800 steel as measured under the experimental flow curve and predicted using RVEs of different sizes, and (b) with an enlarged scale

The flow curve of DP800 steel was accurately predicted up to the onset of macroscopic plastic instability and the ultimate tensile strength of the steel was predicted with less than 0.3% error.

REFRENCES

[1] ASTM E112, 2013, Standard Test Methods for Determining Average Grain Size. Abbaschian, R., Abbaschian, L., and Reed-Hill, R. E., 2008, Physical metallurgy principles,Cengage Learning, Stamford, CT, US.
[2] ASTM E8/E8M, 2013, Standard Test Methods for Tension Testing of Metallic Materials.
[3] Al-Abbasi, F. M., and Nemes, J. A., 2003, "Micromechanical modeling of dual phase steels," Int. J. Mech. Sci., **45**(9), pp. 1449–1465.
[4] Al-Abbasi, F. M., and Nemes, J. A., 2003, "Micromechanical modeling of the effect of particle size difference in dual phase steels," Int. J. Solids Struct., **40**(13-14), pp. 3379–3391.
[5] Al-Abbasi, F., 2004, "Micromechanical Modeling of Dual Phase Steels", PhD Dissertation, McGill University.
[6] Ajmal, M., Tindyala, M. A., and Priestner, R., 2009, "Effect of controlled rolling on the martensitic hardenability of dual phase steel", Int. J. Miner. Metall. Mater., **16**(2), pp. 165– 169.
[7] Buessler, P., 1999, ECSC steel RTD first report.
[8] Bergstrom, Y., 1970, "A dislocation model for the stress-strain behaviour of polycrystalline α-Fe with special emphasis on the variation of the densities of mobile and immobile dislocations," Materials Science and Engineering, **5**(4), pp. 193–200.
[9] Bouaziz, O., Irsid, P. B., Group, U., and Usinor, G., 2002, "Mechanical behaviour of multiphase materials : an intermediate mixture law without fitting parameter," pp. 71–77.
[10] Balliger, N. K., and Gladman, T., 1981, "Work hardening of dual-phase steels", Met. Sci., **15**, pp. 95–108.
[11] Bhadeshia, H. K. D., 2001, Bainite in steels, transformation, microstructure and properties, Institute of Materials, London, UK.
[12] Bhadeshia, H. K. D. H., 1990, "Model for transition from upper to lower bainite", Materials Science and Technology, **6**, pp. 592–603.
[13] Bourell, D. L., and Rizk, a., 1983, "Influence of martensite transformation strain on the ductility of dual-phase steels", Acta Metall., **31**(4), pp. 609–617.

ISSN: 2277-9655
Impact Factor: 4.116
CODEN: IJESS7

[14] Bag, A., Ray, K. K., and Dwarakadasa, E. S., 1999, "Influence of martensite content and morphology on tensile and impact properties of high-martensite dual-phase steels", Metall. Mater. Trans. A, **30**(5), pp. 1193–1202.
[15] Byun, T. S., and Kim, I. S., 1993, "Tensile properties and inhomogeneous deformation of ferrite-martensite dual-phase steels", J. Mater. Sci., **28**(11), pp. 2923–2932.
[16] Brands, D., Schröder, J., Balzani, D., Dmitrieva, O., and Raabe, D., 2011, "On the Reconstruction and Computation of Dual-Phase Steel Microstructures Based on 3D EBSD Data," Proc. Appl. Math. Mech., **11**(1), pp. 503–504.
[17] Balliger, N.K., Gladman, T., 1981. Work hardening of dual-phase steels. Met. Sci., **15**(3), 95– 108
[18] Committee on International Iron & Steel Institute Committee on Automotive Applications, 2006, "Advanced high strength steel (AHSS) application guidelines", Available: http://autotechnika.hu/archiv/AHSS.pdf, DOA: 11/30/2014.
[19] Durand-Charre, M., 2004, Microstructure of Steels & Cast Irons (Engineering Materials and Processes), Springer, Berlin, Germany.
[20] Gil Sevillano, J., 1993, "Flow stress and work hardening," Plastic Deformation of Materials, H. Mughrabi, ed., Weinheim (FRG), pp. 19–88.
[21] Gladman, T., 1997, The Physical Metallurgy of Microalloyed Steels, The Institute of Materials,The University Press, Cambridge, London.
[22] Gündüz, S., 2009, "Effect of chemical composition, martensite volume fraction and tempering on tensile behaviour of dual phase steels", Mater. Lett., **63**(27), pp. 2381–2383.
[23] Hollomon, J. H., 1945, "Tensile Deformation," Trans. AIME, **162**, pp. 269–290.
[24] Hall, E. O., 1951, "The Deformation and Ageing of Mild Steel: III Discussion of Results", Proc. Phys. Soc. Sect. B, **64**(9), pp. 747–753
[25] Hwang, B.-C., Cao, T.-Y., Shin, S. Y., Kim, S.-H., Lee, S.-H., and Kim, S.-J., 2005, "Effects of ferrite grain size and martensite volume fraction on dynamic deformation behaviour of 0·15C–2·0Mn–0·2Si dual phase steels", Mater. Sci. Technol., **21**(8), pp. 967–975.
[26] Hill, R., 1963, "Elastic properties of reinforced solids: some theoretical principles," J. Mech. Phys. Solids, **11**, pp. 357–372.
[27] Hill, R., 1984, "On macroscopic effects of heterogeneity in elastoplastic media at finite strain," Math. Proc. Cambridge Philos. Soc., **95**, pp. 481–494.
[28] Ishikawa, N., Parks, D. M., Socrate, S., and Kurihara, M., 2000, "Micromechanical modeling of ferrite-pearlite steels using finite element unit cell models," ISIJ Int., **40**(11), pp. 1170– 1179.
[29] Kouznetsova, V., 2002, "Computational homogenization for the multi-scale analysis of multi-phase materials," Eindhoven University of Technology, The Netherlands.
[30] Kouznetsova, V., Geers, M. G. D., and Brekelmans, W. a. M., 2002, "Multi-scale constitutive modelling of heterogeneous materials with a gradient-enhanced computational homogenization scheme," Int. J. Numer. Methods Eng., **54**(8), pp. 1235–1260.
[31] Kumar, A., Singh, S. B., and Ray, K. K., 2008, "Influence of bainite/martensite-content on the tensile properties of low carbon dual-phase steels," Mater. Sci. Eng. A, **474**(1-2), pp. 270–282.
[32] Kim, S., and Lee, S., 2000, "Effects of martensite morphology and volume fraction on quasistatic and dynamic deformation behavior of dual- phase steels", Metall. Mater. Trans. A, **31**(7), pp. 1753–1760.
[33] Krauss, G., 1978, "Martensitic Transformation, Structure and Properties in Hardenable Steels", Hardenability Concepts With Applications to Steel, D.V. Doane and J.S. Kirkaldy, eds., AIME, Warrendale, PA, pp. 229–248.
[34] Kang, S.-M., and Kwon, H., 1987, "fracture behavior of intercritically treated complex structure in medium-carbon 6Ni steel", Metall. Trans. A, **18**(9), pp. 1587–1592.
[35] Lewis, A. C., and Geltmacher, A. B., 2006, "Image-based modeling of the response of experimental 3D microstructures to mechanical loading," Scr. Mater., **55**(1), pp. 81–85.
[36] Llewellyn, D. T., and Hudd, R. C., 1998, Steels : Metallurgy and Applications, Reed Educational and Professional Publishing Ltd., London, UK.
[37] Liedl, U., Traint, S., and Werner, E. a., 2002, "An unexpected feature of the stress–strain diagram of dual-phase steel", Comput. Mater. Sci., **25**(1-2), pp. 122–128.
[38] Leslie, W. C., 1991, The physical metallurgy of steels, TechBooks, Herndon, Virginia, US.
[39] Mazinani, M., and Poole, W. J., 2007, "Effect of Martensite Plasticity on the Deformation Behavior of a Low-Carbon Dual-Phase Steel," Metall. Mater. Trans. A, **38**(2), pp. 328–339.
[40] Mori, T., and Tanaka, K., 1973, "Average stress in matrix and avegare elastic energy of materials with misfitting inclusions," Acta Metall., **21**, pp. 571–574.

ISSN: 2277-9655
Impact Factor: 4.116
CODEN: IJESS7

[41] Marvi-Mashhadi, M., Mazinani, M., and Rezaee-Bazzaz, A., 2012, "FEM modeling of the flow curves and failure modes of dual phase steels with different martensite volume fractions using actual microstructure as the representative volume," Comput. Mater. Sci., **65**, pp. 197–202.
[42] Nemat-Nasser, S., 1999, "Averaging theorems in finite deformation plasticity," Mech. Mater., **31**, pp. 493–523.
[43] Paul, S. K., 2013, "Real microstructure based micromechanical model to simulate microstructural level deformation behavior and failure initiation in DP 590 steel," Mater. Des., **44**, pp. 397–406.
[44] Pareige, P., 2013, "Irradiation effects in structural components of nuclear reactor: an experimental nanoscale point of view". Available: http://mecamat2013.lmgc.univmontp2.fr/presentations.htm, DOA: 11/30/2014.
[45] Petch, N. J., 1953, "The cleavage strength of polycrystals", J. Iron Steel Inst., **174**, pp. 25-28
[46] Pickering, F. B., 1978, Physical Metallurgy and the Design of Steels, Applied Science Publishers LTD, London.
[47] Paul, S. K., 2013, "Effect of material inhomogeneity on the cyclic plastic deformation behavior at the microstructural level: micromechanics-based modeling of dual-phase steel," Model. Simul. Mater. Sci. Eng., **21**(5), p. 058001.
[48] Paul, S. K., and Kumar, A., 2012, "Micromechanics based modeling to predict flow behavior and plastic strain localization of dual phase steels," Comput. Mater. Sci., **63**, pp. 66–74.
[49] Rashid, M. S., 1981, "Dual Phase Steels", Annu. Rev. Mater. Sci., **11**(1), pp. 245–266.
[50] Ramazani, a., Mukherjee, K., Prahl, U., and Bleck, W., 2012, "Modelling the effect of microstructural banding on the flow curve behaviour of dual-phase (DP) steels," Comput. Mater. Sci., **52**(1), pp. 46–54.
[51] Ramazani, A., Mukherjee, K., Abdurakhmanov, A., Prahl, U., Schleser, M., Reisgen, U., and Bleck, W., 2014, "Micro–macro-characterisation and modelling of mechanical properties of gas metal arc welded (GMAW) DP980 steel," Mater. Sci. Eng. A, **589**, pp. 1–14.
[52] Ramazani, A., Mukherjee, K., Quade, H., Prahl, U., and Bleck, W., 2013, "Correlation between 2D and 3D flow curve modelling of DP steels using a microstructure-based RVE approach," Mater. Sci. Eng. A, **560**, pp. 129–139.
[53] Rodriguez, R., and Gutierrez, I., 2003, "Unified formulation to predict the tensile curves of steels with different microstructures," Mater. Sci. Forum, **426-432**(5), pp. 4525–4530.
[54] Ramazani, A., Pinard, P. T., Richter, S., Schwedt, A., and Prahl, U., 2013, "Characterisation of microstructure and modelling of flow behaviour of bainite-aided dual-phase steel," Comput. Mater. Sci., **80**, pp. 134–141.
[55] Sodjit, S., and Uthaisangsuk, V., 2012, "Microstructure based prediction of strain hardening behavior of dual phase steels," Mater. Des., **41**, pp. 370–379.
[56] Samei, J., 2013, "Multi-scale Characterization of Hyperplasticity and Failure in Dual Phase Steels Subject to Electrohydraulic Forming", PhD Dissertation, University of Windsor.
[57] Smallman, R. E., and Bishop, R. J., 1999, Modern Physical Metallurgy and Materials Engineering, Butterworth-Heinemann, Oxford, UK.
[58] Spiech, G. R., and Wadimont, H., 1968, "Yield Strength and Transformation Substructure of Low-Carbon Martensite", Iron Steel Inst., **206**, pp. 385–392.
[59] Speich, G. ., and Miller, R. L., 1979, "Mechanical Properties of Ferrite-Martensite Steels", Structure and Properties of Dual-Phase Steels, R.A. Kot, and I. Morris, eds., TMS-AIME, New York, pp. 145–182.
[60] Speich, G. R., and Miller, R. L., 1979, "Mechanical properties of ferrite-martensite steels", in Structure and properties of dual-phase steels, American Institute of Mining, Metallurgical, and Petroleum Engineers, pp. 145–182.
[61] Sodjit, S., and Uthaisangsuk, V., 2011, "High Strength Dual Phase Steels and Flow Curve Modeling Approach," The Second TSME International Conference on Mechanical Engineering, Krabi, Thailand.
[62] Sodjit, S., and Uthaisangsuk, V., 2012, "A micromechanical flow curve model for dual phase steels," J. Met. Mater. Miner., **22**(1), pp. 87–97.
[63] Sluis, O. Van Der, Schreurs, P. J. G., Brekelmans, W. A. M., and Meijer, H. E. H., 2000, "Overall behaviour of heterogeneous elastoviscoplastic materials: effect of microstructural modelling," Mechanics of Materials, **32**, pp. 449-462.
[64] Thomser, C., Uthaisangsuk, V., and Bleck, W., 2009, "Influence of martensite distribution on the mechanical properties of dual phase steels: experiments and simulation", Steel Research International, **80**(8), pp. 582-587.
[65] Terada, K., Hori, M., Kyoya, T., and Kikuchi, N., 2000, "Simulation of the multi-scale convergence in computational homogenization approaches," Int. J. Solids Struct., **37**(16), pp. 2285–2311.

ISSN: 2277-9655
Impact Factor: 4.116
CODEN: IJESS7

[66] Uthaisangsuk, V., Prahl, U., and Bleck, W., 2011, "Modelling of damage and failure in multiphase high strength DP and TRIP steels", Eng. Fract. Mech., **78**(3), pp. 469–486.
[67] Williams, E. W., and Davies, L. K., 1963, "Recent developments in annealing", ISI Spec. Rep. 79
[68] Waterschoot, T., Cooman, B. C., and Vanderschueren, D., 2001, "Influence of run-out table cooling patterns on transformation and mechanical properties of high strength dual phase and ferrite–bainite steels", Ironmaking and steelmaking, **28**(1), p. 185-190.
[69] Winchell, P. G., and Cohen, M., 1962, "The Strength of Martensite", Trans. ASM, **33**, pp. 347–361.
[70] Zeytin, H. K., Kubilay, C., and Aydin, H., 2008, "Investigation of dual phase transformation of commercial low alloy steels: Effect of holding time at low inter-critical annealing temperatures", Mater. Lett., **62**(17-18), pp. 2651–2653.